



Received on 02 July 2024; received in revised form, 10 August 2024; accepted, 24 October 2024; published 01 December 2024

DEVELOPMENT, CHARACTERIZATION, AND EVALUATION OF TOPICAL GEL FORMULATED WITH LULICONAZOLE-LOADED SOLID LIPID NANOPARTICLES

Prankshi Sharma¹, Lovely Chourisia¹ and Vijay Kumar^{*2}

Department of Pharmaceutics¹, IIMT College of Medical Sciences, IIMT University Meerut - 250001, Uttar Pradesh, India.

Department of Pharmaceutics², School of Pharmaceutical Education & Research (SPER), Jamia Hamdard - 110062, New Delhi, India.

Keywords:

Solid lipid nanoparticles (SLN),
Luliconazole, Anti-fungal activity,
Topical gel formulation, Fungal
infections

Correspondence to Author:

Vijay Kumar

Research Scholar,
Department of Pharmaceutics,
School of Pharmaceutical Education
& Research (SPER), Jamia Hamdard -
110062, New Delhi, India.

E-mail: vijaypharma1997@gmail.com

ABSTRACT: Luliconazole is an antifungal medication effective against various fungi, especially filamentous fungi like dermatophytes. This study aimed to develop a topical drug delivery system for luliconazole to reduce the active drug dose, improve patient compliance, minimize side effects, and enhance local absorption and activity. Solid lipid nanoparticles (SLNs) were formulated using stearic acid and poloxamer 188 via the solvent diffusion method to address luliconazole bioavailability barriers. The developed SLN and gel formulations underwent physicochemical testing, in-vitro drug release profiles, and kinetics studies. Successful formulation was confirmed by FTIR spectroscopy and scanning electron microscopy. SLN formulation F1 showed significant entrapment efficacy of 96.87 ± 0.009 . The SLNs exhibited unimodal size distribution with a polydispersity index of 0.168, intercept value of 0.98 with 92% peak intensity, and zeta potential of 18.8 mV. The mean particle diameter was 344.3 nm. The G3 gel formulation, containing 1.5% w/v carbopol 934, demonstrated superior entrapment efficacy of 91.39 ± 0.187 . It also exhibited a sustained release profile, with $79.57 \pm 0.213\%$ of the medication released after 24 hours. These findings suggest that the topical administration of luliconazole-loaded SLN-based gel with 1.5% w/v carbopol 934 may offer enhanced antifungal efficacy.

INTRODUCTION: Fungal infections typically impact every system of the body and result in the death of the body's cellular systems. Chronic fungal infection causes subcutaneous mycosis, which is a fungus infection affecting the dermis and subcutaneous tissue. Sporotrichosis, caused by the fungus *Sporothrix schenckii*, is one of the most common tropical illnesses.

To stop the progression of a fungal infection, the treatment must be exceedingly effective while causing minimal side effects. The only approach to managing a fungal infection's progressive spread is to give the patient a palliative choice. However, a variety of topical treatments for treating fungal infections of the skin and subcutaneous tissue are commercially available.

Pharmaceutical formulations include things like creams and lotions. Because of the bioavailability barrier or a shortage of drugs at the treatment site, patient compliance is a major issue^{1, 2}. Given the importance of local antifungal therapy, the absorption rate of the drug should be adjusted based on the kind of agent in order to provide

<p>QUICK RESPONSE CODE</p> 	<p>DOI: 10.13040/IJPSR.0975-8232.15(12).3531-47</p> <hr/> <p>This article can be accessed online on www.ijpsr.com</p> <hr/> <p>DOI link: https://doi.org/10.13040/IJPSR.0975-8232.15(12).3531-47</p>
---	--

sufficient therapeutic value and offer extended pharmacological effects. Individual medication administration is required for fungal infections that affect the epidermis, dermis and deeper layers of the skin in order to localize high drug concentrations in the epidermal and dermal layers. Although luliconazole topical treatments (1 percent weight/volume cream luliconazole) are associated with decreased skin retention of medication³. The introduction of new species of fungi over time is characterized by fungal infection, which causes major health problems in vulnerable individuals with high morbidity and mortality rates. In many cases, it's associated to hematologic allogeneic prolonged leukopenia and autologous grafts disease (patients). Fungal skin infection is currently one of the world's most serious dermatological concerns. Around 40 million people have been infected with fungi in poor and undeveloped countries, according to study^{4,5}.

Dermatophytes are one of the most common causes of tinea and onychomycosis. Applicant Infections are also one of the most common fungi that affect the skin. Topical infection treatment is an effective way for treating both local and systemic infections. A well-known treatment for local skin illness is medication delivery to the skin. This allows active compounds to penetrate the epidermis and improve absorption. Local medication administration, which is metabolized in the first step, is one of the most successful delivery methods. It works well against fungal infections in general. The benefits of administering medications through the skin include less side effects, steady drug delivery, non-invasiveness, convenience of administration, and termination. Topical drug delivery is challenging, however, because the skin acts as a barrier to drug delivery and drug transit through the skin is a complicated process⁶.

Solid lipid nanoparticles (SLNs) have emerged as a cutting-edge, modern-day novel drug delivery device (NDDS). Solid Lipid Nanoparticles were first found in 1991 and are colloidal vehicles that include polymeric and nano, liposomal emulsions, and nanoparticles^{7,8}. Improved drug penetration capacity, targeted drug delivery, a strong release profile, good physical stability, and minimal degradability are all benefits of the contemporary SLN method⁹.

Nanoparticles having sizes of 10 to 1000 nm have been found to boost medicine bioavailability. Compiling a dashboard with SLNs is a significant feature in the era of colloidal drug delivery systems that generate different particles in the field of NDDS¹⁰. Solid lipid nanoparticles are a new kind of drug carrier nanoparticles that are gaining a lot of attention as topical drug carriers. The size of SLN is submicron, and it contains medically suitable lipid components that are solid at normal temperature. SLN overcomes restrictions by combining the advantages of polymeric nanoparticles, lipid emulsions, and liposomes. Biodegradable and biocompatible solid lipid nanoparticles are used for accurate targeting and regulated pharmaceutical distribution. Specialized carriers include creams, tinctures, and emulsions, controlled release, minimal skin irritation, and active component protection are all benefits of SLN.

Specialized carriers include creams, tinctures, and emulsions, Controlled release, minimal skin irritation, and active component protection are all benefits of SLN. Solid lipid nanoparticles, in particular, can improve skin penetration, provide a prolonged release to avoid systemic absorption, and function as a UV sunscreen to lessen skin irritation. The skin reacts to SLN in a particular way. The most efficient lipid based colloidal carrier is solid lipid nanoparticle (SLN), which was discovered in the early 1990s and created utilizing high pressure homogenization (HPH) or micro-emulsion technology. The encapsulated substance can be protected from chemical degradation and drug release can be altered thanks to the solid matrix of the particles¹¹. Luliconazole is an antifungal drug having an imidazole moiety and a dithioacetate ketone that works against a variety of fungus, including filamentous fungi like dermatophytes¹².

Although the particular mechanism of action of this novel antifungal medicine is unknown, luliconazole has been proven to inhibit fungal cytochrome P450. The enzyme 14- α -demethylase prevents the generation of ergosterol from lanosterol and interferes with the development of fungal cell walls¹³. Luliconazole is a broad-spectrum antifungal medication that has been approved by the FDA. Because of the bioavailability barrier, luliconazole does not obstruct the topical system.

For fungal infections, the cutaneous and subcutaneous layers must individualize the drug's permeability, allowing high quantities of the drug to be administered at the therapeutics' point of action. However, because a variety of topical luliconazole formulations with reduced skin permeability and a short skin retention time are available on the market, patient compliance is good¹⁴. Nano drugs have experienced an exponential expansion in the pharmaceutical industry because of their high drug loading capacity, restricted excipients, drug durability, and little damage, easy scaling, and processing complexity. The low water solubility of luliconazole prevents skin absorption and makes topical administration difficult. Medication solubility in the lipid phase of the stratum corneum further restricts penetration¹⁵.

A gel is a "semi-solid system" that consists of a liquid phase and a polymer matrix with a high degree of physical and chemical cross-linking. A gel is a three-dimensional interconnected two-component network made up of a structural substance dispersed in a sufficient yet significant amount of liquid to form an exceedingly stiff network structure. Inorganic particles and organic macromolecules, particularly polymers, are commonly found in the structural elements that make up a gel network. Crosslinking is typically caused by chemical or physical interactions. As a result, gels are divided into two categories: chemical and physical gel systems¹⁶.

MATERIALS AND METHODS:

Reagents and Chemicals: Luliconazole was provided as a gift sample from SMS Pharmaceuticals India, Stearic acid was purchased from Fisher Scientific India Pvt. Ltd, Carbopol-934 was purchased from sigma Aldrich, Italy, while Ethanol was purchased from Merck, India, n-octanol was purchased from SD Fine-chem. Ltd, Mumbai, and Methanol purchased from Fisher Scientific India Pvt. Ltd, Poloxomer 188 purchased from central drug house Ltd, Potassium Dihydrogen orthophosphate, sodium hydroxide, and Disodium hydrogen orthophosphate purchased from Thomas baker New Delhi.

Preformulation Studies:

Determination of Maximum Absorption of Luliconazole in Ethanol: Determined the

luliconazole absorption maximum using a modified procedure. A stock solution containing 1 mg/ml of luliconazole was produced in methanol. Next, luliconazole concentrations of 2, 4, 6, 8, and 10 mg/ml are obtained by serial dilution, and a UV spectrophotometer set to 299 nm wavelength is used for analysis¹⁷.

Determination of Lipophilicity: The evaluation of lipophilicity was conducted using the conventional shake flask method. Three distinct volumetric flasks were each filled with the necessary quantity of luliconazole. And then measured amount of lipids such as precinol, stearic acid, dynasan-114 were placed into each flask. The resulting heterogeneous mixture is vortexed and agitated for 48 hours at 37°C and 50 rpm. After the supernatant was removed and filtered using a 0.22µm syringe filter, it was subjected to spectrophotometric analysis at a wavelength of 299 nm additionally ascertain the luliconazole partition coefficient using the water and n-octanol partition systems¹⁸. A conical flask containing the measured amount of luliconazole was filled with the measured amounts of n-octanol and aqueous buffer solution. To establish equilibrium, the flask was stirred for 48 hours. The resulting mixture was transferred to a separating funnel and left to separate two layers for 45 minutes. Each layer's first component was taken and examined using a UV spectrophotometer set at 299nm. The resulting value of both phases was determined and log₁₀ P of ration was calculated¹⁹.

Determination of Aqueous Solubility: The aqueous solubility of luliconazole was determined by the saturation shake flask process. A large quantity of luliconazole was dissolved in distilled water and acetate buffer (pH) then shaken at 50rpm at 37°C for 48 hours, filtered in the solution, and analyzed at λ_{max} of 299nm by UV spectroscopy²⁰.

Fourier Transformation Infrared Spectroscopy: SLN G3 underwent FTIR analysis utilizing a Win-IR and a Bio-Rad FTS spectrophotometer. Potassium bromide was used to collect individual samples, and spectroscopy was performed on them in the 4000-400 cm⁻¹ range²¹.

Preparation of Solid Lipid Nanoparticle with Luliconazole: The solid lipid nanoparticle (SLNs) were prepared using the solvent diffusion method.

A known quantity of luliconazole and stearic acid were added to 5ml ethanol and heated from $65\pm 3.0^{\circ}\text{C}$ in the water bath. The resulted solution was added into 5ml aqueous poloxomer 188 solutions at $4-6^{\circ}\text{C}$ with magnetic stirring at 2000rpm using a syringe. Solid lipid nanoparticle formed instantly and was recovered by centrifugation at 2000rpm for 30 min at 4°C . The resultant heterogeneous mixture then proceeded to high-pressure homogenization (HPH) using APV 2000 homogenizer at 1200 bars. The resultant mixture was placed at room temperature and turned into transparent nanocrystals through recrystallization of dispersed lipid¹⁴.

Evaluation of Solid Lipid Nanoparticle:

Physicochemical Property: Color, odor, pH, and the solubility of SLN F3 in aqueous media were used to investigate the physicochemical features of the SLN dispersions²².

Entrapment Efficiency: Entrapment efficiency of solid lipid nanoparticle with Luliconazole (LUL) was determined by described process with some changes. Solid lipid nanoparticle were prepared at 37°C . Take 5mg dried solid lipid nanoparticle was dissolved in 10 ml ethanol and then filtered by a syringe filter $0.22\mu\text{m}$ size. Analyzed the concentration of Luliconazole spectrophotometrically at 299nm. Entrapment efficiency was determined by the following equation.

$$\% \text{ Entrapment Efficiency (EE)} = \frac{W(\text{initial drug}) - W(\text{free drug})}{W(\text{initial drug})}$$

Where, $W_{(\text{initial drug})}$ is the mass of drug added initially, $W_{(\text{free drug})}$ is the mass of free drug detected after centrifugation²³.

Optical Microscopic Analysis: The optical microscopy analysis of determine solid lipid nanoparticle F3 composition, the analysis was performed at 100x magnification using a digital optical microscope with a fluorescent lamp (labomed Lx-400). It is used to determine if Luliconazole solid lipid nanoparticles are efficiently localized with uniform texture in solid lipid nanoparticle(SLN) dispersion²⁴.

Zeta Potential Measurement and Particle size Analysis: The described approach was used to determine the zeta potential and particle size. The

analysis was performed at 37°C by a zeta potential or particle size analyzer. Solid lipid nanoparticle F3 was diluted with phosphate buffer saline solution and maintained the pH of the solution at 7.4 and then analyzed the sample²⁵.

Fourier Transform Infrared Spectroscopy for SLN F3: FTIR analysis for solid lipid nanoparticle (SLN) F3 determined by Win IR, Bio-Rad FTS spectrophotometer, each sample mixed with potassium bromide and later proceed for the spectroscopical and observed from 4000 to 400 cm^{-1} ²⁶.

Optimization of Prepared SLN-Luliconazole:

DoE: The optimization of Solid Lipid Nanoparticles (SLN) was carried out using the Design of Expert (DoE) software version 132.0.4 by Stat-Ease, based in Minneapolis, MN, USA. This software facilitated the optimization of batches according to predefined independent and dependent variables. In this formulation, Particle Size (PS), Entrapment Efficiency (EE), and Drug Loading (DL) were the primary independent variables and dependent responses under investigation.

Ternary phase diagrams were utilized to determine the optimal levels for oil and surfactant concentrations, crucial for the DoE. These diagrams helped in selecting high, medium, and low concentrations for the independent variables. The chosen optimization strategy was the Box–Behnken design (BBD), a type of response surface methodology known for predicting how independent variables affect dependent responses. The implementation of the Box–Behnken design involved 17 randomized runs, allowing for a thorough exploration of the experimental conditions and ensuring an effective and reliable optimization of SLN batches to improve particle size, entrapment efficiency, and drug loading²⁷.

Development and Evaluation of Gel: The gel base was first created by dissolving carbopol 934P in a specified amount of distilled water at 600rpm, then adding propyl paraben sodium (0.1 % w/v) and methyl paraben (0.02 % w/v) and stirring constantly for half hour. The prepared gel base was set aside for 24 hours. Secondly, solid lipid nanoparticle (SLN) F3 was dispersed with the

appropriate amount of 1% ethanol (20% w/w) and propylene glycol (5% w/w) and later added to carbopol gel bases with continuous stirring at 1000 rpm and followed by agitation for 30 min. To maintain a pH of 5.5-6.5 for best efficacy, TEA (Tri-ethanol amine) was added to the final step and thoroughly agitated to obtain a clear uniform gel. Some procedure was applied to obtain four formulations with different quantities of carbopol and the aim in relation to the production of various gel forms was to obtain the best homogenous and uniformly texture with stable physico-chemical reliability in terms of percentage of the release of major constituents²⁸. The various formulations of solid lipid nanoparticle gels are listed in the **Table 1**.

TABLE 1: DIFFERENT PREPARED GEL FORMULATION CONTAINING SOLID LIPID NANOPARTICLE

Formulations code	Carbopol 934 % (w/w)
G ₁	0.5
G ₂	1
G ₃	1.5
G ₄	1.8

Texture Analyzer: The firmness, cohesiveness, consistency, and viscosity of the NEG sample were evaluated using a texture analyzer (TA. Plus, Stable Micro Systems, Surrey, UK) in compression mode. The resulting force–time graphs provided data that was used to determine several mechanical properties of the NEG sample^{29,30}.

Determination of Entrapment Efficiency: Entrapment efficiency of each prepared batches of gel was determine by measuring the free mass of drug in diffuse phase of gel solution after centrifugation. Briefly, 1gm gel dispersed with ethanol and stirred for 5min. Then, the resulting mixture was centrifuged at 15000 rpm for 1 hour at 4°C. The supernatant was collected from centrifuged and analyzed spectrophotometrically at 299nm for quantitative analysis³¹.

Determination of pH: A digital pH meter was used to measure the gel's pH. The pH of the created SLN gel formulation was evaluated by immersing the electrode glass of a pH meter in it and rotating it³².

Determination of Viscosity: The viscosity to the gel was measure using a Brookfield Viscometer.

The viscosity of each gel batches was determined at 50 and 100 rpm and compared with selected desired viscosity range³³.

FTIR Analysis of SLN G₃: FTIR analysis of SLN G₃ was performed using Win-IR spectrophotometer, Bio-Rad FTS spectrophotometer. Individual samples were taken with potassium bromide and then proceed for spectroscopic examination in the range of 4000-400 cm⁻¹³⁴.

SEM (Scanning Electron Microscopy): Morphological analysis of G₃ SLN was determined using scanning electron microscopy according to standard protocols with minor modification. A small quantity of sample of SLN gel was placed on glass slide and dried under vacuum. Then, slide having sample placed in SEM chamber coated with gold-palladium, and after that sample was analyzed under a microscope at an accelerating voltage of 10 Kv³⁵.

Spreadability: The gel's spreadability was assessed using the previously described methodology, with a few modifications. In short, a second plate was positioned concentrically on top of the 500 mg formulation that had been calculated and placed in the center of the acrylic plate.

The primary width was calculated as the diameter of the circle that the gel was applied to. For a few minutes, the plate was subjected to an approximate 500g weight. Gel scattering caused a rise in diameter, which was used to determine the dispersion of gel. The resulting diameter of the dispersed gel was then measured³⁶.

Drug Release and Kinetic Profile: The *in-vitro* drug release profiling approach using dialysis bag techniques was used to assess the drug release and kinetics profiling of the gel with optimized formulation (SLN G₃). One gram of the gel sample was precisely weighed and then put into a cellulose dialysis membrane.

The membrane was secured with threads and placed into a flask containing a 50 milliliter solution of phosphate buffer and ethanol. The container was set up with a magnetic stirrer set at 37 degrees Celsius and 50 revolutions per minute. After that, 1 ml of the sample was taken out at

intervals of 0.5, 1, 1.5, 2, 3, 4, 5, 6, 8, 12, and 24. At the same time as the sample was taken out, dissolving medium was added back to the removal quantity. Spectrophotometric measurements were made at 299 nm to determine the mass release from luliconazole entrapped in SLN. Three measurements of each were made.

The Higuchi, Zero order, First order, and Korsmeyer-Peppas models are among the kinetic models that were used to statistically assess the *in-vitro* release profile of the prepared solid lipid nanoparticle gel containing luliconazole. A kinetic model was established to clarify the drug release profile's process. Regression coefficients that are

high are seen to be particularly useful for initialization and acceptability³⁷.

RESULTS AND DISCUSSION:

Preformulation Study of Drug:

Optimization of the Absorption Maximum of LUL (Luliconazole) in Ethanol: The regression equation and coefficient for the drug absorption established using a technique utilizing absorption maximum of Luliconazole at wavelength 299nm versus concentrations 2-10 µg/ml, were found to be $0.1353x + 0.043$ and 0.9996 respectively. The goal of this study is to determine Luliconazole absorption maximum and validate the process for qualitative and quantitative analysis³⁸.

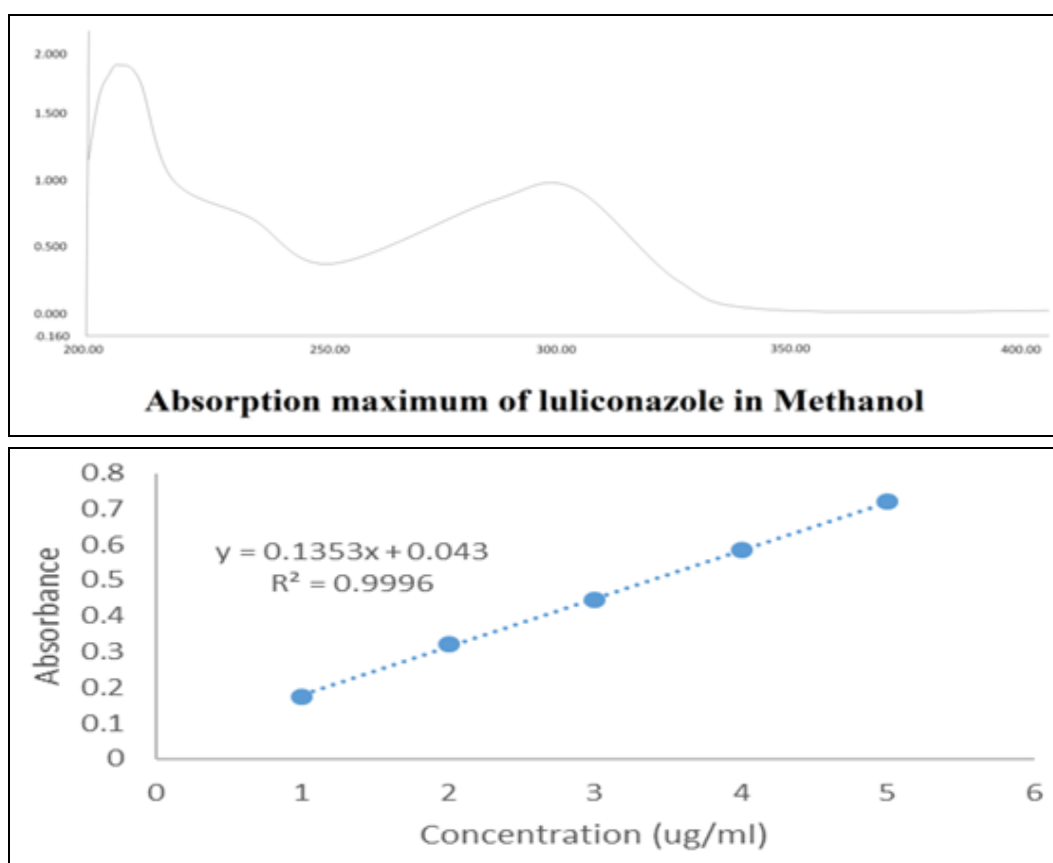


FIG. 1: ABSORPTION MAXIMA OF LULICONAZOLE AND REGRESSION COEFFICIENT AGAINST THE DIFFERENT CONCENTRATION OF LULICONAZOLE

Physicochemical tests of Luliconazole were conducted to assess the drug's physicochemical properties and to determine its hydrophilic and lipophilic compatibility.

The solubility of Luliconazole in water was determined to be 0.00586 ± 0.294 mg/ml whereas solubility in stearic acid, prectrol, dynasan 114 was found to be 23.755 ± 0.49 , 18.315 ± 0.86 , and

22.877 ± 0.34 mg/ml. In addition, non-aqueous solubility of Luliconazole in n-octanol obtained 17.985 ± 0.53 mg/ml.

Luliconazole had $\log_{10} P$ values of 3.99, 3.90, 3.28 and 3.68 in stearic acid, dynasan 114, prectrol and n-octanol respectively. The compatibility of the leading moiety was investigated using FTIR analysis of Luliconazole and stearic acid before and

after formulation. **Fig. 2** shows the FTIR spectroscopy of Luliconazole; **Table 1** lists the main IR absorption peaks of Luliconazole at 2986.24 cm^{-1} (C-H stretch), 2206.24 cm^{-1} ($\text{C}\equiv\text{N}$ stretch), 1560.56 cm^{-1} (C-H aromatics stretch), 1476.54 cm^{-1} (C=C-C aromatic ring stretch),

827.62 cm^{-1} (para C-H distribution) and 760.27 cm^{-1} (C-Cl stretch).

The purity and validity of luliconazole were confirmed by these identified main peaks, as described in this report³⁹.

TABLE 2: FTIR INTERPRETATION OF LULICONAZOLE

Characteristics peaks	Reported (cm^{-1})	Observed (cm^{-1})
C-H stretch	2500 – 3000	2986.24
$\text{C}\equiv\text{N}$ stretch	2100- 2400	2206.24
C =C aromatic stretch	1400-1600	1560.56
C=C-C aromatic ring stretch	1500-1400	1476.54
Para C-H distribution	850-800	827.62
C-Cl stretch	600-800	760.27

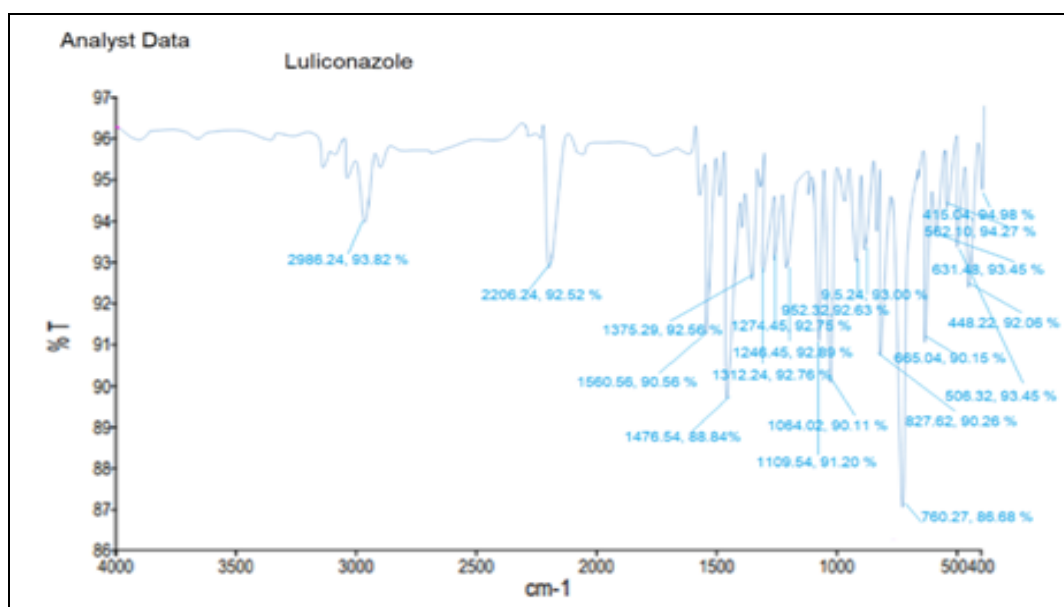


FIG. 2: FTIR SPECTRA OF LULICONAZOLE

Fig. 3 and **Table 3** show the FTIR spectra for stearic acid and interpretation. Infrared absorption principle maxima of stearic acid were revealed in the spectra at 2925.28 cm^{-1} (C-H stretch alkanes), 2858.24 cm^{-1} (C-H stretch aldehyde), 1710.54 cm^{-1} (C=O stretch saturated), 1481.52 cm^{-1} (C-C stretch), 1305.32 cm^{-1} (C-O stretch, aromatic aster),

946.59 cm^{-1} (O-H bend), 730.00 cm^{-1} (C=C bend) and 557.28 cm^{-1} (C-I stretch).

The purity and authenticity of stearic acid were confirmed by these identified primary peaks, which were similar to those reported³⁹.

TABLE 3: FTIR INTERPRETATION STEARIC ACID

Characteristics peaks	Reported (cm^{-1})	Observed (cm^{-1})
C-H stretch alkanes	2800-3000	2925.28
C-H stretch aldehyde	2500-2800	2858.24
C=O stretch saturated	1700-1750	1710.54
C- C stretch	1400-1500	1481.52
C-O stretch, aromatic aster	1250-1350	1305.32
O-H bend	900-950	946.59
C=C bend	665-750	730.00
C-I stretch	500-600	557.28

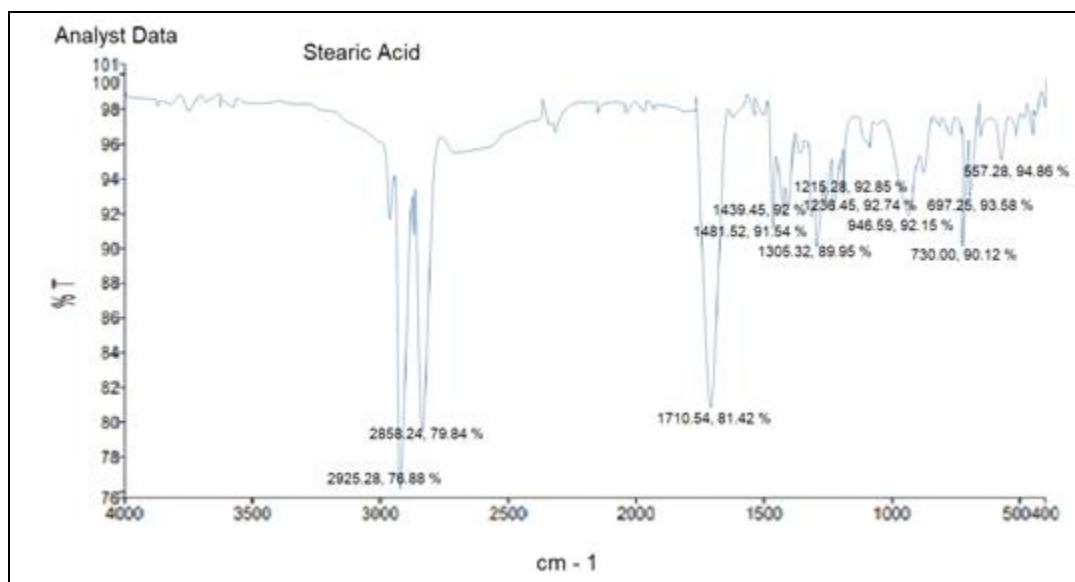


FIG. 3: FTIR SPECTRUM OF STEARIC ACID

Preparation Method of Luliconazole Containing Solid Lipid Nanoparticle: This approach uses multiple modified nano-precipitation process for determination of solid lipid nanoparticle in respect of entrapment efficacy of Luliconazole at both treatment divisions, *i.e.*, cooling sonication probe and nano-precipitation. The temperature is set in both segments at 4°C and 25°C. The instantaneous addition of organic phase to the aqueous phase is kept at 4°C resulting direct precipitation due to anti-solvent hyphenation. During the nano-precipitation phase, the temperature is regulated, which aids homogeneity.

Reduces the size of larger crystals and aggregation during bead milling, which helps high pressure homogenizers achieve consistent homogeneity¹⁴. Furthermore, the procedure is stored step by step with different adjustments in stearic acid and poloxomer 188(w/v) concentrations in the range of 0.5-2% in SLN optimization. The percent entrapment of the active moiety was determined spectrophotometrically at 299nm for all of the produced SLN groups. The results were statistically assessed, and a solid lipid nanoparticle with high Luliconazole entrapment was chosen as the optimal SLN for evaluations.

TABLE 4: PREPARATION OF LULICONAZOLE SOLID LIPID NANOPARTICLE

Code for SLN	SLN formation with various concentration of leading reagents		
	Luliconazole % (w/v)	Poloxomer 188% (w/v)	Stearic % (w/v)
F1	1	1	0.5
F2	1	1	0.7
F3	1	1	1
F4	1	1	2
F5	1	0.5	1
F6	1	1.5	1
F7	1	2	1

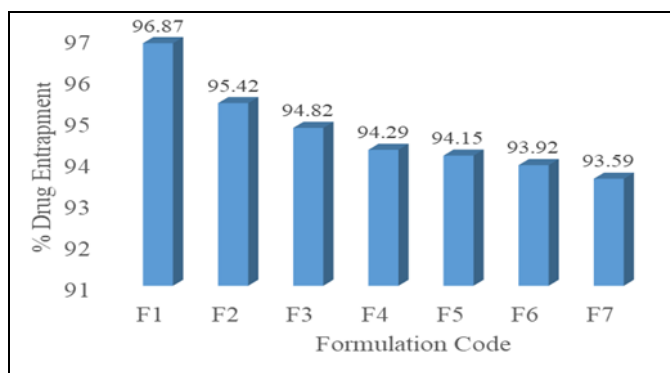
Evaluation of SLN:

Evaluation of Entrapment Efficiency (EE) of SLN: The physicochemical and spectroscopic properties of Luliconazole were first determined. Following the successful development of several nanoparticle baths, the percentage entrapment efficiency of Luliconazole was evaluated at 299nm, the percentage of entrapment efficiency was measured spectrophotometrically. Following that, with Luliconazole content of 96.87 ± 0.009 and

93.59 ± 0.001 (w/w), SLN F1 and SLN F7 have the highest and lowest percent EE of SLN, respectively. In a study quoted by Ige *et al.*, the maximum percentage EE was reported to be 90-96% (w/w)¹⁴. As a result, SLN F3 was chosen as an optimal SLN based on percent drug entrapment and it was tested further for physicochemical and gel forming properties. Fig. 4 depicts the percent drug entrapment of SLN batches graphically.

TABLE 5: PERCENTAGE ENTRAPMENT EFFICIENCY OF SLN

Formulation code	Percentage Entrapment (mean \pm SD)
F1	94.87 \pm 0.009
F2	95.42 \pm 0.002
F3	96.82 \pm 0.0005
F4	94.29 \pm 0.001
F5	94.15 \pm 0.002
F6	93.92 \pm 0.004
F7	93.59 \pm 0.001

**FIG. 4: PERCENTAGE ENTRAPMENT EFFICIENCY (EE) OF LULICONAZOLE IN SOLID LIPID NANOPARTICLE**

Physicochemical Property: The physicochemical properties of SLN F3 were assessed, including color, odor, pH stability and water solubility. The physicochemical results revealed that the SLN has white clear color with a homogeneous and uniform texture, aromatic odor, stability at 7.4 pH and water solubility of 0.01829 ± 0.036 mg/ml, which significantly higher than that of Luliconazole.

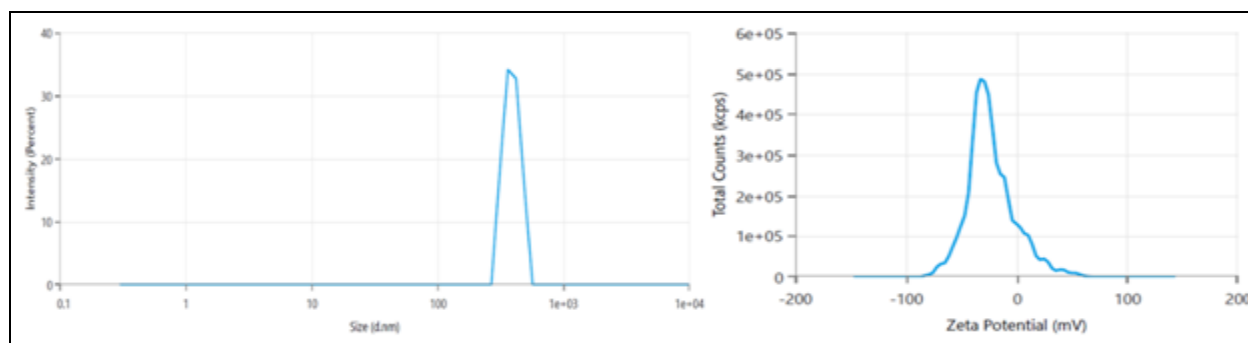
Optical Microscopy: Optical microscopy of optimized preparation, SLN was performed using at a magnification of 100X using a digital light optical microscope, and observations revealed that Luliconazole SLN was effectively localized inside the SLN dispersion with a homogenous and uniform texture. Only particles with an average diameter bigger than $2.5 \mu\text{m}$ could be seen clearly

under a microscope, according to the study. Furthermore, there was no assembled structure in the SLN preparation. In optical microscope pictures of SLN F3 containing Luliconazole displayed in **Fig. 5**, the micellar structure was not visible.

**FIG. 5: OPTICAL MICROSCOPY PICTURE OF LULICONAZOLE CONTAINING SLN F3**

Zeta Potential and Particle size Distribution Identification:

The nano ZS90 zetasizer device was used to successfully determine particle size analysis and zeta potential measurements of SLN with Luliconazole. The Zeta potential is a key measure for predicting nanoparticle physical stability. The stability of a nanoparticle system is determined by the zeta potential, which suggests that the nanosystem is more stable since it provide a deterrent force between nanoparticles⁴⁰. **Fig. 6** indicates that a solid lipid nanoparticle with a zeta potential of -23.15mV has a high value of zeta potential, indicating that the nanosystem is stable. Solid lipid nanoparticle had a mean particle diameter by $\sim 362.8\text{nm}$, unimodal size distribution, polydispersity index (PDI) 0.169, intercept value 0.99 and peak intensity 92% in particle size analysis. If the polydispersity is less than 0.5, the polydispersity index shows the diffusion factor with little nanoparticle aggregation⁴¹.

**FIG. 6: PARTICLE SIZE, ZETA POTENTIAL AND SIZE DISTRIBUTION OF LULICONAZOLE SLN F3**

Comparability Study of Drug Excipients using FTIR: A FTIR analysis of solid lipid nanoparticle F3 was carried out to examine into probable drug-excipients interaction. The absorption peaks of Luliconazole were found to be 3478.23 cm^{-1} for C-H stretching, 2623 & 2547 cm^{-1} for S-H stretching, 2046.07 cm^{-1} for $\text{C}\equiv\text{N}$ stretching, 1915.88 cm^{-1} for C=N stretching, 1608.02 cm^{-1} for C=C aromatic ring stretching and 980.06 cm^{-1} for C-CI stretching in the spectrum data. In the high frequency range,

primary absorption of stearic acid was discovered at stearic at 3178.60 cm^{-1} & 3040.06 cm^{-1} attributed to $-\text{CH}_2$ band symmetric and asymmetric stretching vibrations, respectively and in the low frequency range 1840.86 is attributed to $-\text{COOH}$ vibrations. After successful SLN production, spectral analysis of determined SLN indicated that there was no change in Luliconazole. The spectral data strongly support the reported referenced value⁴².

TABLE 6: FOURIER TRANSFORM INFRARED SPECTROSCOPY INTERPRETATION OF SLN F3

Characteristics peaks	Reported (cm^{-1})	(Observed cm^{-1})
C-H stretch	3000-3500	3478.23, 3178.60, 3040.06
$\text{C}\equiv\text{N}$ stretch	2100-2400	2046.07
C=C alkene stretch	1600-2000	1840.86
C=C aromatic stretch	1450-1650	1608.02
C-CI stretch	600-1000	980.06

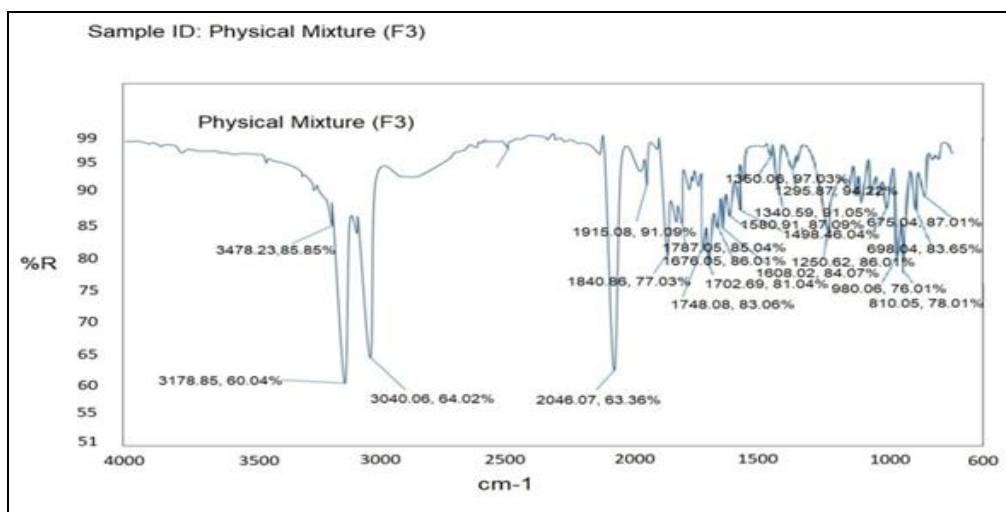


FIG. 7: FTIR SPECTRA OF SOLID LIPID NANOPARTICLE F3

BBD: Mathematical Model Fitting and Optimization of Solid Lipid Nanoparticle F3: In the current formulation, the selected independent variables are oil concentration (%), Smix ratio (%), and sonication time (s). The dependent responses are particle size (nm), polydispersity index, and drug loading (DL) (%). Ternary phase diagrams were used to determine the high, medium, and low levels of oil and surfactant concentrations necessary for the Design of Experiments (DoE). The optimization design employed was the Box-Behnken Design (BBD), a response surface

methodology used to predict the effects of independent variables on dependent responses **Table 7**. The varied levels or experimental ranges for the selected independent variables are detailed in Table 8. It was noted that all three dependent responses fit a polynomial quadratic model, with a non-significant lack of fit ($p > 0.05$) **Table 4**. The results of the BBD were displayed as 3D response surface graphs **Fig. 3** to illustrate the interaction between each dependent response and two different independent variables. The following sections provide detailed descriptions of each response.

TABLE 7: BBD-BASED SOLID LIPID NANOPARTICLE F3 WITH INDEPENDENT AND DEPENDENT VARIABLES

Steric acid Conc.	Poloxomer Conc.	Starring speed	Size	EE	DL
0.5	0.5	2000	397.7	73.52	0.416
0.5	1.25	1500	374.1	73.52	0.392
0.5	1.25	2500	366.2	75.89	0.38

0.5	2	2000	314.5	96.53	0.315
1.25	0.5	1500	483.9	50.41	0.602
1.25	0.5	2500	469.6	56.78	0.547
1.25	1.25	2000	405.1	65.18	0.443
1.25	1.25	2000	409.7	70.29	0.435
1.25	1.25	2000	412.6	73.52	0.432
1.25	1.25	2000	412.6	73.52	0.432
1.25	1.25	2000	412.6	73.52	0.432
1.25	2	1500	349.6	89.01	0.352
1.25	2	2500	329.8	91.16	0.331
2	0.5	2000	496.4	47.58	0.64
2	1.25	1500	475.3	52.01	0.58
2	1.25	2500	414.1	63	0.459
2	2	2000	324.4	93.31	0.325

TABLE 8: SELECTED INDEPENDENT VARIABLES AND THEIR LEVELS

Name	Goal	Lower Limit	Upper Limit	Lower Weight	Upper Weight	Importance
A: Steric acid conc.	is in range	0.5	2	1	1	3
B: Poloxomer Conc.	is in range	0.5	2	1	1	3
C: Sterring speed	minimize	1500	2500	1	1	3
Size	minimize	314.5	496.4	1	1	3
EE	maximize	47.58	96.53	1	1	3
DL	maximize	0.315	0.64	1	1	3

TABLE 9: REGRESSION ANALYSIS SUMMARY FOR RESPONSES (PARTICLE SIZE IN NM), (EE), AND (DL)

Quadratic Model	%CV	R ²	Adjusted R ²	Predicted R ²	SD
Particle size	0.0036	0.998	0.9795	0.8693	0.0047
Entrapment Efficacy (EE)	0.0025	0.997	0.9603	0.938	0.0038
(DL)	0.0039	0.999	0.9859	0.9096	0.0032

$Size = 410.52 + 32.2125 * A + -66.1625 * B + -12.9 * C + -22.2 * AB + -13.325 * AC + -1.375 * BC + -14.035 * A^2 + -13.235 * B^2 + 10.94 * C^2$
 $EE = 71.206 + -7.945 * A + 17.715 * B + 2.735 * C + 5.68 * AB + 2.155 * AC + -1.055 * BC + 0.397 * A^2 + 6.132 * B^2 + -5.498 * C^2$
 $DL = 0.4348 + 0.062625 * A + -0.11025 * B + -0.026125 * C + -0.0535 * AB + -0.02725 * AC + 0.0085 * BC + -0.008025 * A^2 + -0.002775 * B^2 + 0.025975 * C^2$

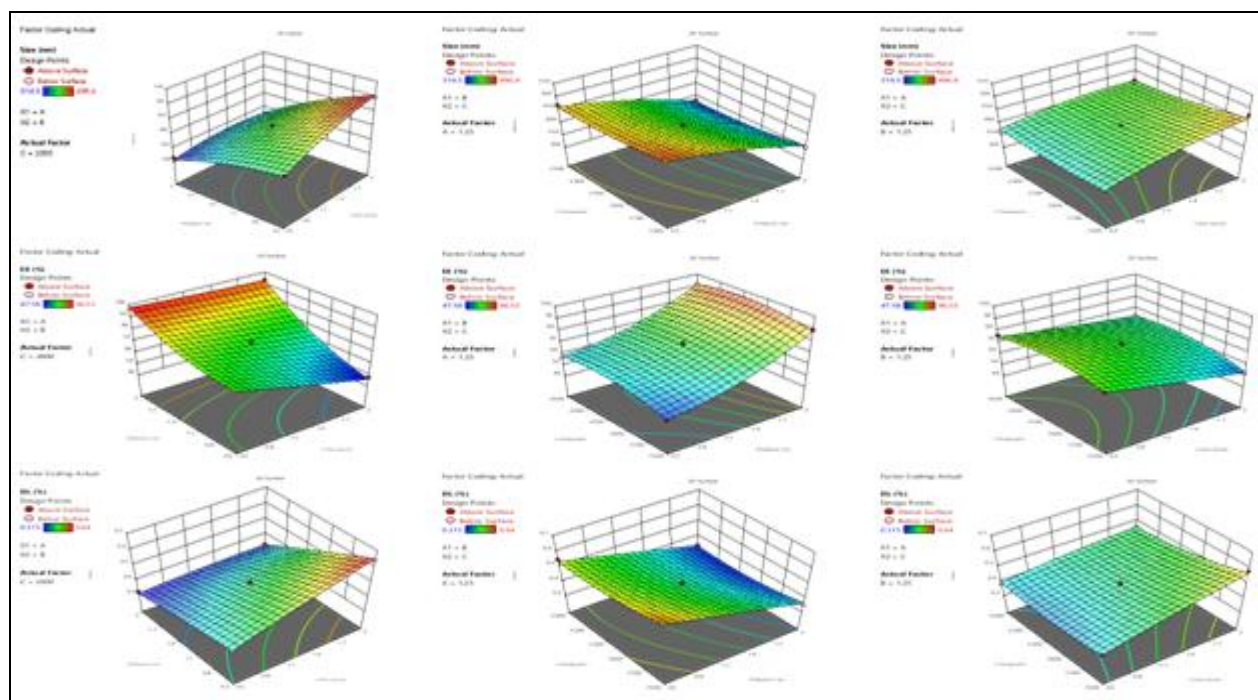


FIG. 8: 3D RESPONSE SURFACE DEPICTING THE INTERACTION EFFECT OF THE INDEPENDENT VARIABLES LIKE OIL, SMIX, SONICATION TIME ON PARTICLE SIZE, EE, AND % DL

Optimization and Evaluation of SLN Gel: Using the stirring method and carbopol 934P as the gelling agent, a topical gel containing SLN loaded with Luliconazole was successfully synthesized. The method for preparing various SLN gels was found to be simple and reliable. To determine % entrapment of Luliconazole, the four distinct preparations of SLN gel categorized as G₁, G₂, G₃, and G₄ were initially spectrophotometrically analyzed at 299nm. The results show that SLN G₃ with 1.5% carbopol w/w has the highest percentage of drug entrapment at 91.38±0.187%. After that,

physiochemical parameters like visual appearance, pH, viscosity, and spread ability are checked on the optimized formulation. The viscosity of the G₃ gel is 369cP, which is equivalent to the gel viscosity reported by jana *et al*, and the pH is 6.13±0.254 according to the results. In terms of spreadability, the prepared SLN gel has a spreadability factor of 4.5, indicating that it has outstanding spreadability as a topical formulation. From the perspective of patient compliance, spreadability is a key physical property of any topical formulation⁴³.



FIG. 9: VISUAL APPEARANCE OF SLN G₃

Analysis of the Texture of Both the Placebo and the Formulation: The textural properties, depicted in Fig. 10, were assessed for both the placebo and the optimized formulations. For the optimized SLN gel F3, cohesiveness was determined to be -27.78 g, showing its capacity to adhere when subjected to tensile stress. Firmness was found to be -41.09 g,

indicating its resistance to compressive force and maintaining its structural integrity. Furthermore, consistency was measured at 393.98 g.sec, and the viscosity index was -213.90 g.sec, highlighting the formulation's stability, suitability for packaging, and ease of use⁴⁴.

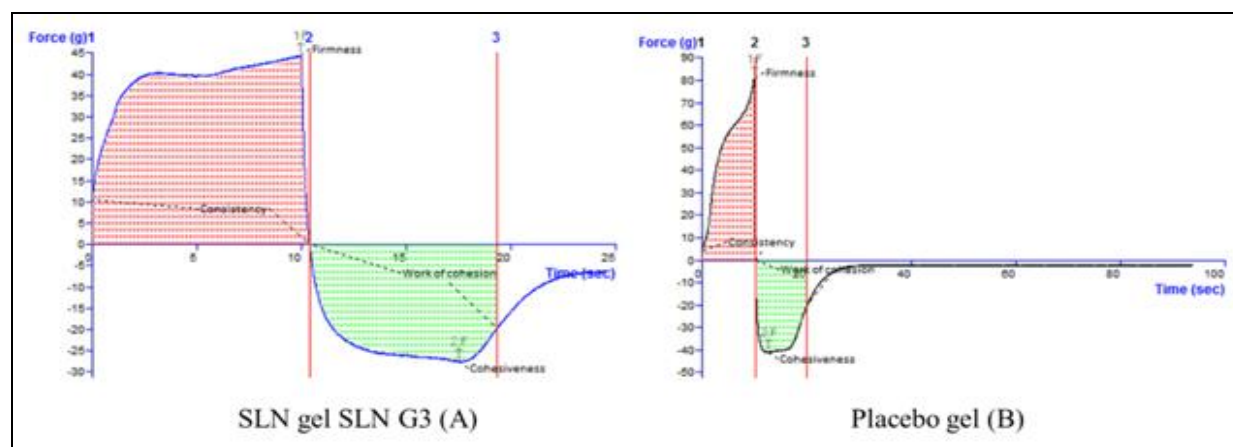


FIG. 10: TEXTURE ANALYSIS OF THE SLN GEL F3 FORMULATION (A) AND PLACEBO GEL (B)

In-vitro Drug Release and Kinetics Study:

Foretelling release mechanisms and comparing release profiles are common applications of statistical modeling. To measure the drug's *in-vitro* release profile in a buffer system for a whole day, the dialysis bag technique was employed.

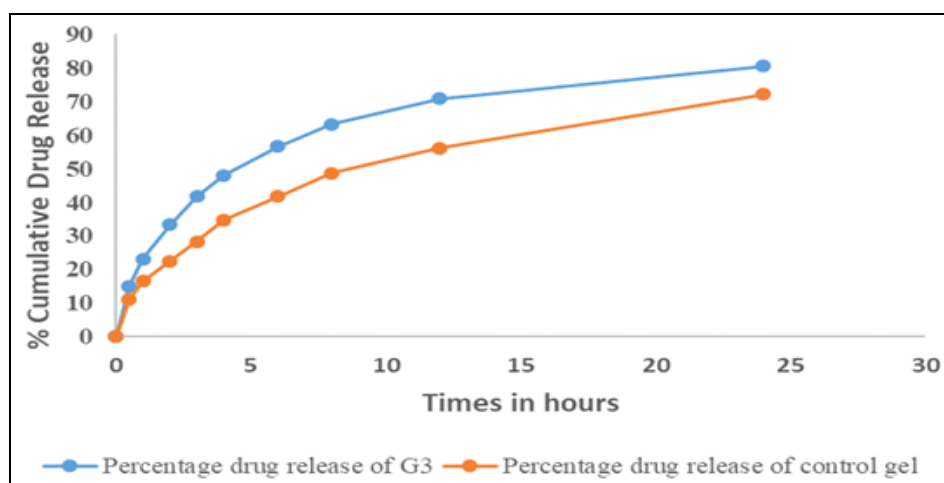
Fig. 11 and **Table 10** demonstrate how the percentages of luliconazole that have been desolated from SLN rise over time. Evidence from the release profile demonstrates that the developed SLN is able to release medications under controlled conditions. Because most SLN forms exhibit homogeneous drug trapping throughout the system, the leading moiety can be released gradually. Ekambaram *et al.* put out a similar idea, asserting that when the drug is evenly dispersed throughout the lipid matrix, a controlled drug desolation profile

can be achieved. Poloxomer 407 is significantly more effective than Cremophor RH 40 at preventing drug release from SLN due to its higher HLB value. 20 Poloxomer 407 has a high degree of external spreadability, hence mitigating the impact of interfacial tension that may arise between the dissolving medium and SLN.

Additionally, it decreases the accumulation of drug particles, hastening the decomposition of medications. Additionally, the lipid mass of SLN can be utilized to modify the size of nanoparticles and enhance the strength of drug delivery. A prolonged time of drug distribution is produced when the lipid surrounding the nanoparticle thickens, extending the period of drug disassociation⁴⁵.

TABLE 10: PERCENTAGE DRUG RELEASE PROFILE OF G₃ AND CONTROL GEL

Sr. no.	Time in hours	Percentage drug release of G ₃	Percentage drug release of control gel
1	0	0	0
2	0.5	15.005 ± 0.002	11.076 ± 0.851
3	1	23.069 ± 0.013	16.470 ± 0.618
4	2	33.382 ± 0.021	22.506 ± 0.067
5	3	41.685 ± 0.006	28.326 ± 0.050
6	4	48.056 ± 0.003	34.800 ± 0.147
7	6	56.678 ± 0.015	41.770 ± 0.282
8	8	63.335 ± 0.064	48.680 ± 0.401
9	12	70.928 ± 0.103	56.226 ± 0.050
10	24	80.588 ± 0.078	72.270 ± 0.252

**FIG. 11: IN-VITRO DRUG PROFILE OF SLN GEL AND CONTROL GEL**

Furthermore, several kinetic models (zero order, first order, Higuchi, and Krosmyer Peppas model) for the ideal formulation made use of an *in vitro* drug release profile. A statistical analysis was conducted on the obtained data to determine the rate constant and the strongest correlation with the

drug release state kinetics profile. In all models, the best-fitted line was discovered, where it was judged to be unsuitable. The results may explain why pharmaceuticals spread more slowly and how they are distributed in a regulated or regular way from homogenous matrix systems. As a viable topical

formulation for long-term pharmaceutical delivery, the results show that SLN G₃ is significantly more efficacious⁴⁶. As evidenced by prior shards of data, this conclusion is essentially identical to the

virtuous covenant. **Fig. 9** provides a graphical representation of the SLN G₃ gel's kinetics sequence **Fig. 12**.

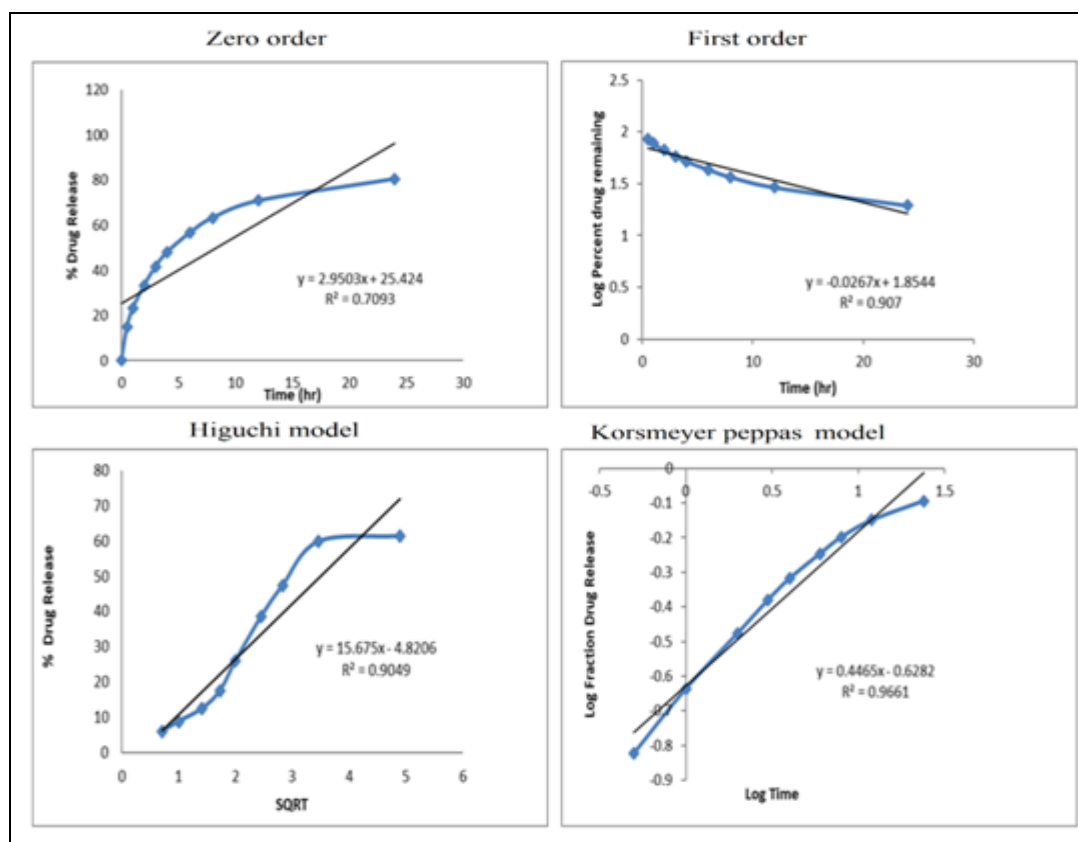


FIG. 12: KINETIC ORDER OF SLN G₃ GEL

TABLE 11: KINETIC ORDER OF SLN G₃ GEL

Formulation	Zero order		First order		Higuchi		Korsmeyer-Peppas	
	R ²	K ₀	R ²	K ₀	R ²	K ₀	R ²	K ₀
SLN gel	0.7093	3.122	0.907	-0.027	0.9049	17.143	0.9661	0.523

FTIR Spectral Analysis of SLN G₃ Gel: The FTIR spectrum analysis of SLN gel G₃ was effective in assessing potential drug-drug additive interactions since it produced spectral data matching stearic acid and luliconazole. Luliconazole's absorption peaks were found at 3340.78 cm⁻¹ for N-H stretching, 2971.30 cm⁻¹ for C-H stretching, 2193.49 cm⁻¹ for C-N stretching, and 818.07 & 1053.28 cm⁻¹ for C-Cl stretching, according to spectral analysis. The primary absorption peaks of stearic acid were identified at 1639.31 cm⁻¹ in the low frequency zone for –COOH stretching vibrations and 2932.49 cm⁻¹ in the high frequency area for asymmetric and symmetric stretching vibrations in the –CH₂-band, respectively. Spectral analysis of improved formulation G₃ revealed no likely interaction

between medication and various additives, even after topical gel was produced consecutively. Consequently, the spectra demonstrate the purity and dependability of the SLN G₃ gel.

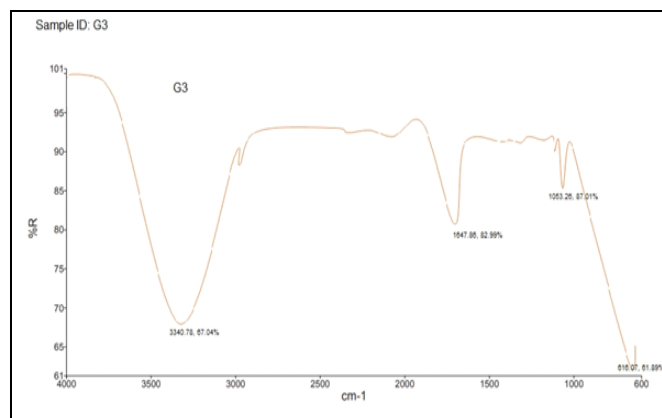
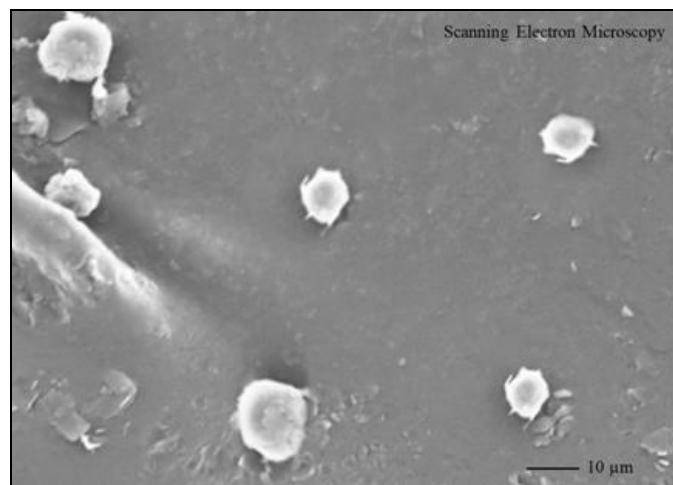


FIG. 13: FTIR SPECTRA OF SLN G₃ GEL

TABLE 12: FTIR INTERPRETATION OF SLN G₃ GEL

Characteristics Peaks	Reported (cm ⁻¹)	Observed (cm ⁻¹)
N-H stretch	3500-3000	3340.78
C=C stretch	1500-2000	1647.80
CO-O- CO stretch	1040-1050	1053.28
C-Cl stretch	550-850	818.07

Scanning Electron Microscopy (SEM): Fig. 14 shows the shape of the improved formulation as confirmed by SEM analysis. The majority of vesicles are well defined, spherical, and discrete, with plenty of internal aqueous space. SEM analysis reveals a low density of nanoparticles, which could be due to dilution of the nano suspension prior to taking SEM picture. According to SEM analysis, the Luliconazole containing SLN in the gel had a spherical form and a smooth surface⁴⁷.

**FIG. 14: SCANNING ELECTRON MICROSCOPY ANALYSIS OF SLN G₃ GEL**

CONCLUSION: By using the solvent diffusion approach Luliconazole loaded solid lipid nanoparticle were successfully created. There was determined to have 92.14±0.978 entrapment efficiency. 2.5μm was found to be the average size of the developed formulation F3. The size of the SLN grew along with the amount of lipid. The compatibility of the medicine and excipients is strongly suggested by FTIR. The Luliconazole loaded SLN G₃ gel formulation with carbopol 934 (1.5% w/v) are optimized as an optimal formulation and acceptable for topical use according to the findings of the current study.

Author Contributions: Conceptualization, methodology, investigation, data curation and writing, P.S; project administration, V.K.; resources and supervision, V.K.; software and

validation, P.S.; writing review and editing and formal analysis, V.K.; supervision, resources, and visualization, L.C. All authors have read and agreed to the published version of the manuscript.

ACKNOWLEDGMENT: The authors would like to thank IIMT College of Medical Science, IIMT University, Meerut, Uttar Pradesh, India and Department of Pharmaceutics, School of Pharmaceutical Education & Research, Jamia Hamdard, New Delhi-110062.

CONFLICT OF INTERESTS: Declare none.

REFERENCES:

- Gou Y, Hu Y and Wang W: Immunotherapy for Fungal Infections. Chinese Journal of Applied Clinical Pediatrics 2024.
- Fang W, Wu J, Cheng M, Zhu X, Du M, Chen C, Liao W, Zhi K and Pan W: Diagnosis of invasive fungal infections: challenges and recent developments. Journal of Biomedical Science 2023; 30(1): 42.
- Mendonça A, Santos H, Franco-Duarte R and Sampaio P: Fungal infections diagnosis - past, present and future. Research in Microbiology 2022; 173(3): 103915.
- Wiederhold NP: Emerging fungal infections: new species, new names, and antifungal resistance. Clinical Chemistry 2021; 68(1): 83–90.
- Rawson TM, Antcliffe DB, Wilson RC, Abdolrasouli A and Moore LSP: Management of Bacterial and Fungal Infections in the ICU: Diagnosis, Treatment, and Prevention Recommendations. Infection and Drug Resistance 2023; 16: 2709–2726.
- Gnat S, Łagowski D, Nowakiewicz A and Dyląg M: A Global view on fungal infections in humans and animals: infections caused by dimorphic fungi and dermatophytoses. Journal of Applied Microbiology 2021; 2688-2704.
- Musiela E, Feliczak-Guzik A and Nowak I: Optimization of the conditions of solid lipid nanoparticles (SLN) Synthesis. Molecules 2022; 27(7).
- Luo WC and Lu X: Solid lipid nanoparticles for drug delivery. In Methods in molecular biology (Clifton, N.J.) 2023; 139–146.
- Ryan A, Patel P, Ratrey P, O'Connor PM, O'Sullivan J, Ross RP, Hill C and Hudson SP: The Development of a solid lipid nanoparticle (sln)-based lactacin 3147 hydrogel for the treatment of wound infections. Drug Delivery and Translational Research 2023.
- Abdelwahab SI, Taha MME, Moni SS and Alsayegh AA: Bibliometric mapping of solid lipid nanoparticles research (2012–2022) using vosviewer. Medicine in Novel Technology and Devices 2023; 17: 100217.
- Paliwal R, Paliwal SR, Kenwat R, Kurmi B. Das and Sahu MK: Solid lipid nanoparticles: a review on recent

- perspectives and patents. Expert Opinion on Therapeutic Patents 2020; 30(3): 179–194.
12. Alhakamy N, Al-Rabia M, Md S, Sirwi A, Khayat S, AlOtaibi S, Hakami R, Al Sadoun H, Eldakhkhny B, Abdulaal W, Aldawsari H, Badr-Eldin S and Elfaky M: Retracted: development and optimization of luliconazole spanlastics to augment the antifungal activity against *Candida albicans*. Pharmaceutics 2021; 13(7): 977.
 13. Dandagi PM, Pandey P, Gadad AP and Mastiholmath VS: Formulation and evaluation of microemulsion based luliconazole gel for topical delivery. Indian Journal of Pharmaceutical Education and Research 2020; 54(2): 293–301.
 14. Yallavula J, Mandava K and Madhav V: Design and evaluation of topical gel containing solid-lipid nanoparticles loaded with luliconazole. International Journal of Pharmacy Research & Technology 2023; 13(2): 52-64.
 15. Gharaghani M, Hivary S, Taghipour S and Zarei-Mahmoudabadi A: Luliconazole, a highly effective imidazole, against fusarium species complexes. Medical Microbiology and Immunology 2020; 209(5): 603-12.
 16. Cao J, Zhang D, Zhou Y, Zhang Q and Wu S: Controlling properties and functions of polymer gels using photochemical reactions. Macromolecular Rapid Communications 2022; 43(4): 2100703.
 17. Lin B, Wang W, Ba W, Li H and Fan J: Preparation and partial pharmacodynamic studies of luliconazole ethosomes. Clinical and Experimental Pharmacology and Physiology 2022; 49(5): 549-57.
 18. Desai NJ and Maheshwari DG: UV Spectrophotometric method for the estimation of luliconazole in marketed formulation (Lotion). Pharma Science Monitor an International J of Pharmaceutical Sci 2014; 5(2): 48-54.
 19. Czyrski A: The spectrophotometric determination of lipophilicity and dissociation constants of ciprofloxacin and levofloxacin. spectrochimica acta part A: Molecular and Biomolecular Spectroscopy 2022; 265: 120343.
 20. Tayyebi A, Alshami AS, Rabiei Z, Yu X, Ismail N, Talukder MJ and Power J: Prediction of organic compound aqueous solubility using machine learning: a comparison study of descriptor-based and fingerprints-based models. Journal of Cheminformatics 2023; 15(1): 99.
 21. Saleem S, Jameel MH, Akhtar N, Nazir N, Ali A, Zaman A, Rehman A, Butt S, Sultana F, Mushtaq M, Zeng JH, Amami M and Althubeiti K: Modification in structural, optical, morphological, and electrical properties of zinc Oxide (ZnO) Nanoparticles (NPs) by Metal (Ni, Co) dopants for electronic device applications. Arabian Journal of Chemistry 2022; 15(1): 103518.
 22. Yang J, Liang Z, Lu P, Song F, Zhang Z, Zhou T, Li J and Zhang J: Development of a luliconazole nanoemulsion as a prospective ophthalmic delivery system for the treatment of fungal keratitis: *In-vitro* and *in-vivo* Evaluation. Pharmaceutics 2022; 14(10): 2052.
 23. Shah N, Prajapati R, Gohil D, Aundhia C, Sadhu P and Kardani S: Luliconazole loaded niosomal topical gel: factorial design, *in-vitro* characterization and antifungal study. Indian Journal of Pharmaceutical Education and Research 2023; 57 (3): 520–527.
 24. Mandal S, Ali SI and Mandal AC: Investigation of structural, optical and photoluminescence properties of the sol-gel synthesized powder ZnS Nanoparticles. Applied Physics A: Materials Science and Processing 2023; 129(3): 219.
 25. Rane BR: Development and *in-vitro* characterization of liposomal gel of bifonazole for topical use. Journal of Medical Pharmaceutical and Allied Sciences 2021; 134–142.
 26. Asadi H, Rostamzadeh K, Salari D and Hamidi M: Preparation of biodegradable nanoparticles of tri-block PLA-PEG-PLA copolymer and determination of factors controlling the particle size using artificial neural network. Journal of Microencapsulation 2011; 28(5): 406–416.
 27. Parashar M and Jain A: Formulation development and evaluation of migraine almotriptan loaded ethosomes using box behnken design. Journal of Pharmaceutical Research International 2021; 214–223.
 28. Chandrakala SG and Srinivasan VS: development and evaluation of micro sponge gel of an antifungal drug. International J of Current Pharmaceutical Research 2023;
 29. Momchilova M, Gradinarska-Ivanova D, Zsivanovits G and Yordanov D: Effect of pork back fat replacement with inulin gel and oat bran flour on the physicochemical and sensory evaluation of a leberkäse meat product. Letters in Applied NanoBioScience 2023; 12(4).
 30. Rashid ANA, Kormin F and Asman S: Quality analysis of meats using fir spectroscopy, colour spectrophotometer, texture analyser and physical image analysis. Journal of Sustainability Science and Management 2021; 16: 103-19.
 31. Dave V, Gupta N, Prakesh A and Sharma P: Improvised strategy of ethanolic nanovesicular gel of phospholipon 90g for transdermal delivery of luliconazole to mitigate fungal diseases. Biomass Conversion and Biorefinery 2023; 13(17): 15463–15469.
 32. Vogel EM, Marques LLM, Droval AA, Gozzo AM and Cardoso FAR: Quality of cosmetics with active caffeine in cream and gel galenic bases prepared by compounding pharmacies. Brazilian J of Biology 2022; 82: 241043.
 33. Pinteá A, Vlad RA, Antonoaea P, Rádai EM, Todoran N, Barabás EC and Ciurba A: Structural Characterization and Optimization of a Miconazole Oral Gel Polymers 2022; 14(22): 5011.
 34. Brambilla E, Locarno S, Gallo S, Orsini F, Pini C, Farronato M, Thomaz DV, Lenardi C, Piazzoni M and Tartaglia G: Poloxamer-Based hydrogel as drug delivery system: how polymeric excipients influence the chemical-physical properties. Polymers 2022; 14(17): 3624.
 35. Datye A and DeLaRiva A: Scanning Electron Microscopy (SEM). In Springer Handbooks 2023; 359-380.
 36. Chow KT, Chan LW and Heng PWS: Characterization of spreadability of nonaqueous ethylcellulose gel matrices using dynamic contact angle. Journal of Pharmaceutical Sciences 2008; 97(8): 3467-82.
 37. Darson J, Thirunellai Seshadri R, Katariya K, Mohan M, Srinivas Kamath M, Etyala MA and Chandrasekaran G: Design development and optimisation of multifunctional doxorubicin-loaded indocyanine green proniosomal gel derived niosomes for tumour management. Scientific Reports 2023; 13(1): 1697.
 38. Jain P, Soni R, Paswan SK and Soni PK: Ketoconazole laden microemulsion based gel formulation against skin fungal infection. International Journal of Applied Pharmaceutics 2023; 15(3): 49-60.
 39. Gumus IB, Kahraman E, Erdol-Aydin N and Nasun-Saygili G: Drug loading of tannic acid crosslinked hydroxyapatite/gelatin composites *via* spray dryer and kinetic studies. Drying Technology 2023; 41(16): 2688-702.
 40. Tang J, Ji H, Ren J, Li M, Zheng N and Wu L: Solid Lipid Nanoparticles with TPGS and Brij 78: A Co-Delivery Vehicle of Curcumin and Piperine for Reversing P-Glycoprotein-Mediated Multidrug Resistance *in-vitro*. Oncology Letters 2017; 13(1): 389-95.

41. Ismail SH, Hamdy A, Ismail TA, Mahboub HH, Mahmoud WH and Daoush WM: Synthesis and characterization of antibacterial carbopol/zno hybrid nanoparticles gel. Crystals 2021; 11(9): 1092.
42. Joshi S, Khatri LR, Kumar A and Rathore AS: NMR based quality evaluation of mab therapeutics: a proof of concept higher order structure biosimilarity assessment of trastuzumab biosimilars. Journal of Pharmaceutical and Biomedical Analysis 2022; 214: 114710.
43. Khoware S, Khan A and Sharma V: Formulation and evaluation of sln based topical gel of ketorolac tromethamine. International Journal of Pharmaceutical Sciences and Medicine 2021; 6(3): 85–109.
44. Huang C, Hu P, Wu Q, Xia M, Zhang W, Lei Z, Li DX, Zhang G and Feng J: Preparation, *in-vitro* and *in-vivo* evaluation of thermosensitive *in-situ* gel loaded with ibuprofen-solid lipid nanoparticles for rectal delivery. Drug Design, Development and Therapy 2022; 16: 1407–1431.
45. Cesur S, Ilhan E, Tut TA, Kaya E, Dalbayrak B, Bosgelmez-Tinaz G, Arisan ED, Gunduz O and Kijeńska-Gawrońska E: Design of cinnamaldehyde- and gentamicin-loaded double-layer corneal nanofiber patches with antibiofilm and antimicrobial effects. ACS Omega 2023; 8(31): 28109-21.
46. Ahmed ASMG and Gowda BHJ: Preparation and evaluation of *in-situ* gels containing hydrocortisone for the treatment of aphthous ulcer. Journal of Oral Biology and Craniofacial Research 2021; 11(2): 269-76.
47. Luo T, Wang C, Ji X, Yang G, Chen J, Janaswamy S and Lyu G: Preparation and characterization of size-controlled lignin nanoparticles with deep eutectic solvents by nanoprecipitation. Molecules 2021; 26(1): 218.

How to cite this article:

Sharma P, Chourisia L and Kumar V: Development, characterization, and evaluation of topical gel formulated with luliconazole-loaded solid lipid nanoparticles. Int J Pharm Sci & Res 2024; 15(12): 3531-47. doi: 10.13040/IJPSR.0975-8232.15(12).3531-47.

All © 2024 are reserved by International Journal of Pharmaceutical Sciences and Research. This Journal licensed under a Creative Commons Attribution-NonCommercial-ShareAlike 3.0 Unported License.

This article can be downloaded to **Android OS** based mobile. Scan QR Code using Code/Bar Scanner from your mobile. (Scanners are available on Google Playstore)